(14) A. Spencer and G. Wilkinson, *J. Chem. Soc., Dalton Trans.*, 786 (1974).
(15) D. F. Christian, G. R. Clark, W. R. Roper, J. M. Waters, and K. R. Whittle, *J. Chem. Soc., Chem. Commun.*, 458 (1972).
(16) C. C. Addison, N. Logan, S. C. Wallwork, and C. D. Gardner *Q. Rev., Chem. Soc.*, **25**, 289 (1971).
(17) M. B. Hursthouse personal communication discussed in ref 3b.
(18) D. M. Barlex and R. D. W. Kemmitt, *J. Chem. Soc., Dalton Trans.*, 1436 (1972).
(19) M. Graziani, R. Ros, and G. Carturan, *J. Organomet. Chem.*, **27**, C19 (1971).
(20) K. Nakamoto, "Infrared Spectra of Inorganic and Coordination Compounds", Wiley-Interscience, New York, N.Y., 1970.
(21) K. Nakamoto, Y. Morimoto, and A. E. Martell *J. Phys. Chem.*, **66**, 346 (1962).
(22) S. D. Robinson and A. Sahajpal *J. Organomet. Chem.*, **99**, C65 (1975).
(23) S. D. Robinson and A. Sahajpal *J. Organomet. Chem.*, **111**, C26 (1976).

Contribution from the Department of Chemistry,
University of Washington, Seattle, Washington 98195

Comparison of Dioxygen and Ethylene as Ligands for Platinum(0)

JOE G. NORMAN, Jr.

Received January 19, 1977 AIC70042L

The results of SCF-Xα-SW calculations on the model chelated-O_2 complex $Pt(PH_3)_2(O_2)$ and its ethylene analogue $Pt(PH_3)_2(C_2H_4)$ are used to discuss the bonding, structure, and reactivity of dioxygen and ethylene complexes. Pt–O_2 and Pt–C_2H_4 covalent bonding is mainly due to mixing of metal $5d_{x^2-y^2}$ and $5d_{z^2}$ orbitals with ligand bonding orbitals of *both* σ and π type. "Back-bonding" in $Pt(PH_3)_2(O_2)$ amounts to essentially complete ionic transfer of two electrons from the Pt $5d_{xy}$ to the in-plane O_2 π^* orbital, with little covalent overlap between the two. However, such overlap is appreciable in $Pt(PH_3)_2(C_2H_4)$, the electrons remaining chiefly in the d_{xy} orbital. $Pt(PH_3)_2(O_2)$ is thus best formulated as a d^8 system (Pt^{II}–O_2^{2-}), and $Pt(PH_3)_2(C_2H_4)$ as a d^{10} system (Pt^0–C_2H_4). By extrapolation, the chelated-O_2 complexes of "d^8" metals are best thought of as d^6 systems (Co^{III}–O_2^{2-}, etc.). The calculations agree well with electronic and x-ray photoelectron spectra. The influence of ligands trans to O_2 or C_2H_4 is used to explain why C_2H_4 is sometimes coordinated in, and sometimes perpendicular to, the molecular plane in complexes and why O_2 is sometimes monodentate and sometimes chelated. The energy-level diagram for $Pt(PH_3)_2(O_2)$ is that of a nucleophile, the HOMO being strongly localized on O_2 as the out-of-plane π^* orbital and the two LUMO's being mainly Pt $5d_{xy}$ and O_2 σ^*, respectively. The mechanisms of SO_2 addition to chelated-O_2 complexes to form coordinated sulfate and the homogeneous catalysis of PPh_3 oxidation by $Pt(PPh_3)_3$ are discussed in these terms. Some Pt 5d → P 3d π back-bonding is observed in the calculated electronic structures, as a replacement of 3s by 3d character in the phosphorus bonding functions. The implications of this result for the general question of metal–phosphorus bonding are discussed.

Introduction

The critical role played by transition metals in both biochemical and industrial processes involving molecular oxygen makes the chemistry of metal–dioxygen complexes especially important. Among the three coordination modes known for dioxygen—monodentate (**1**), bridging (**2**), and chelating

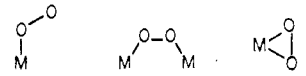

1 2 3

(**3**)—the first has particular significance because it almost certainly occurs (with M = Fe) in oxygenated heme proteins.[1,2] However, the great majority of known dioxygen complexes contain chelated O_2; a recent review[3] lists 43 x-ray structures of type **3** vs. 16 of types **1** and **2** combined.

Chelated-O_2 complexes fall naturally into two main groups: those of early transition metals in high oxidation states (e.g., $[MoOF_4(O_2)]^{2-}$) and those of group 8 metals in lower oxidation states (e.g., $Ir(PPh_3)_2(CO)(Cl)(O_2)$). After several years of discussion, it now seems clear that *both* groups are best formulated as *peroxo* complexes, i.e., as containing O_2^{2-} covalently bound to metals in oxidation states $\geq 2+$.[3-5] Consistently, the range of O–O distances in reliable structures is 1.40–1.52 Å (average 1.45 (2) Å),[3,6] bracketing the value for peroxide ion, 1.49 Å. Though pleasing in its simplicity, this picture clearly does not describe the M–O_2 bonding in enough detail to resolve many important issues. For example, despite the similar structures of the early transition metal and group 8 complexes, the O_2 unit behaves formally as an electrophile in the former and as a nucleophile in the latter.[7,8]

In order to provide a more sophisticated basis for discussing the chemistry of chelated-O_2 complexes in terms of electronic structure, I am carrying out SCF-Xα-SW calculations[9] on representative molecules. To exemplify group 8 complexes, $Pt(PPh_3)_2(O_2)$ [10] is an obvious choice. Its structure is simple and accurately known by x-ray crystallography.[11] It participates in many well-defined reactions,[7,12] sometimes as a homogeneous catalyst,[13] which one might hope to explain. Moreover, it has an exact ethylene analogue, also structurally characterized,[14] allowing a close comparison of the bonding of these two important π ligands. $Pt(PPh_3)_2(C_2H_4)$ is interesting in its own right as the classic example of a d^{10} ethylene complex. This paper presents a comparison of calculations for the model compounds $Pt(PH_3)_2L$, L = O_2, C_2H_4. A very preliminary account of the results for $Pt(PH_3)_2(O_2)$ has appeared.[15]

Experimental and Computational Section

Synthesis and Electronic Spectra. $Pt[P(C_6H_5)_3]_2(O_2)$ was prepared by a published procedure.[10] Electronic spectra for degassed methanol solutions under nitrogen were recorded from 700 to 210 nm using a Cary 14 instrument.

Initial Parameters. Calculations were made on the conformations of C_{2v} symmetry shown below (the molecular plane is *xy*). Bond

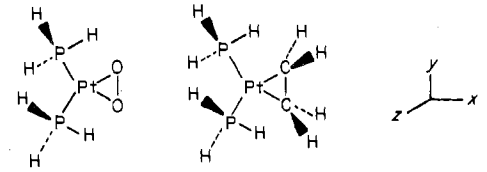

parameters used were Pt–O = 2.006 Å, Pt–P = 2.233 Å, O–O = 1.505 Å, and P–Pt–P = 101.23° for $Pt(PH_3)_2(O_2)$, Pt–C = 2.11 Å, Pt–P = 2.27 Å, C–C = 1.43 Å, C–H = 1.08 Å, P–Pt–P = 111.6°, and H–C–H = 116° for $Pt(PH_3)_2(C_2H_4)$, and P–H = 1.415 Å and H–P–H = 93.45° for both molecules. These were derived from the known structures of $Pt(PPh_3)_2(O_2)$,[11] $Pt(PPh_3)_2(C_2H_4)$,[14] PH_3,[16] and (for the C–H distance and H–C–H angle) $(CH_2)_2O$.[17] A value $\alpha/2$ = 28° for the CC–CH_2 dihedral angle in $Pt(PH_3)_2(C_2H_4)$ was obtained from a least-squares plot of $\alpha/2$ vs. C–C distance for eight alkene complexes for which this angle has been measured. Coordinates in

Table I. Atomic- and Outer-Sphere Radii (bohrs) Used for $Pt(PH_3)_2L$

L = O_2		L = C_2H_4	
Region	Radius	Region	Radius
Pt	2.500	Pt	2.530
O	1.816	C	1.751
P	2.334	P	2.331
H	1.448	H_P[a]	1.439
Outer	7.073	H_C[a]	1.282
		Outer	7.247

[a] H_P and H_C are the hydrogen atoms attached to phosphorus and carbon, respectively.

atomic units to the nearest 0.000 01 bohr were obtained from these bond parameters using the relations 1 bohr = 0.529 17 and 0.529 177 Å for the O_2 and C_2H_4 complexes, respectively.

Schwarz's α_{HF} values[18] were used for the atomic exchange parameters, except for hydrogen, where 0.777 25 was used.[19] For the extramolecular and intersphere regions, a weighted average of the atomic α's was employed, the weights being the number of *valence* electrons in the neutral atoms. The outer-sphere center positions were computed using the same sort of average of the atomic positions. Overlapping sphere radii were obtained by my nonempirical procedure;[20] they are given in Table I.

SCF Calculations. The initial molecular potentials were constructed by superposition of neutral-atom SCF–Xα results. Full C_{2v} symmetry was used to factor the secular matrix. Spherical harmonics through $l = 4$, 2, 1, and 0 were used in the extramolecular, Pt and P, O and C, and H regions, respectively, to expand the wave functions. Core energy levels were never frozen; in each iteration they were calculated explicitly using only the surrounding-atomic-sphere potential. Details of the SCF process are exemplified by the C_2H_4 complex: using a 9:1, 3:1, and 2:1 average of the initial and final potentials for a given iteration to start the next for iterations 1–7, 8–12, and 13–24, respectively, convergence to ±0.000 05 hartree or better was attained for all levels. Each iteration required 1.3 min of CDC 6400 computer time.

Excited and Ionized States. The SCF ground-state potentials were used to search for excited-state levels up to −0.005 hartree. The same potentials were then used as the starting point for calculating electronic transitions and ionization energies using the transition-state procedure.[9b] These calculations were done in spin-restricted form only, so that the values obtained are predictions of the weighted average of singlet and triplet components.

Results

The electronic spectrum of $Pt(PPh_3)_2(O_2)$ in methanol shows one quite distinct shoulder at about 335 nm before onset of strong unresolved absorption that continues upward in intensity to the observational limit of 210 nm. This shoulder was established as a peak maximizing at 29.8×10^3 cm^{-1} (ϵ 1100) using a Du Pont 310 curve resolver.

Table II shows the spherical-harmonic basis functions on Pt and the O_2 or C_2 unit which contribute to each representation of C_{2v} in the chosen coordinate system. The important points to note are that (1) in-plane "forward-donation", from ligand bonding orbitals to the metal, will occur in a_1 levels, (2) in-plane "back-donation" into ligand antibonding orbitals will occur in b_2 levels, and (3) although C_2, like O_2, nominally has out-of-plane π and π^* functions, both in C_2H_4 and $Pt(PH_3)_2(C_2H_4)$ these are tied up in C–H bonding.

The calculated one-electron valence energy levels and charge distribution for both complexes are given in Table III. Inspection of these and wave function contour maps allows one to separate the most important levels for Pt–O_2 and Pt–C_2H_4 bonding—those correlating most closely with Pt 5d and ligand 2p-type σ, π, and π^* orbitals—from the rest. These levels are compared in Figure 1 with those of the free ligands, calculated in the same way and with the same coordinate system as the complexes. The orbitals labeled "σ" and "π" for C_2H_4 are $2a_g$ and $1b_{3u}$, respectively. For comparison, the free-Pt-atom 5d orbital energy is −0.2403 hartree. Omitted from the diagram are the following: (1) the very low-energy O_2 2s-type σ and σ^* orbitals—$1a_1$ and $1b_2$ in the complex; (2) C_2H_4 C–H bonding orbitals—$1a_1$, $2b_2$, $1b_1$, and $2a_2$ in the complex; (3) PH_3 P–H bonding orbitals[20a]—$2a_1$, $2b_2$, $1b_1$, $5a_1$, $1a_2$, and $4b_2$ in $Pt(PH_3)_2(O_2)$ and $2a_1$, $1b_2$, $4a_1$, $2b_1$, $1a_2$, and $3b_2$ in $Pt(PH_3)_2(C_2H_4)$; (4) mainly Pt–P bonding orbitals, correlating with the PH_3 "lone pairs"[20a]—$3b_2$ and $6a_1$ for $Pt(PH_3)_2(O_2)$, $4b_2$ and $5a_1$ for $Pt(PH_3)_2(C_2H_4)$.

Table II. Distribution of Pt and O_2 or C_2 Spherical-Harmonic Basis Functions among Representations of C_{2v}

Representation	Pt functions	O_2 or C_2 functions[a]
a_1	s, p_x, d_{z^2}, $d_{x^2-y^2}$	σ, $\pi_\parallel$
b_2	p_y, d_{xy}	σ^*, $\pi_\parallel{}^*$
b_1	p_z, d_{xz}	$\pi_\perp$
a_2	d_{yz}	$\pi_\perp{}^*$

[a] $\pi_\parallel$ refers to a bonding combination with the *nodal* plane *perpendicular* to the molecular plane; $\pi_\perp{}^*$, to an antibonding combination with the *nodal* plane *in* the molecular plane, etc. See text for coordinate system.

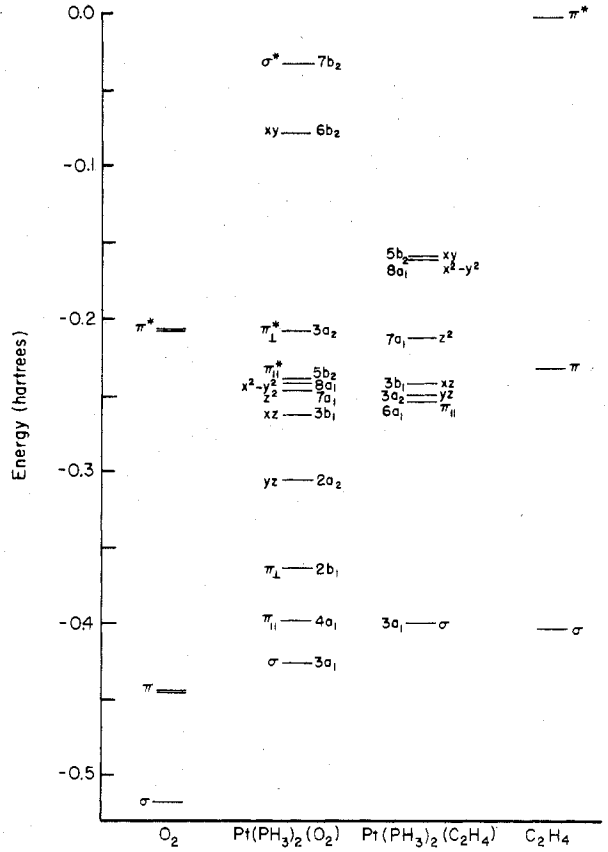

Figure 1. Important Pt–O_2 and Pt–C_2H_4 bonding orbitals of the complexes, compared with corresponding levels of O_2 and C_2H_4. The complex levels are labeled according to the Pt 5d or ligand level with which they most closely correlate.

Wave function contour maps are shown in Figure 2 and also in Figures 3 and 4 (supplementary material) for the most important Pt–O_2 and Pt–C_2H_4 bonding orbitals and in Figure 5 for the main "back-bonding" orbitals. The total valence charge densities are depicted in Figure 6; in Figure 7 are shown the first unoccupied orbital of $Pt(PH_3)_2(O_2)$ and what the charge density would look like if it were occupied.

Table IV summarizes all-electron properties for the two molecules. The atomic charges were estimated by simply normalizing the total number of *valence* electrons within all the atomic spheres to the total number for the molecule. This amounts to partitioning the intersphere and extramolecular charge among the atoms using weights equal to the number

Table III. Valence Energy Levels (hartrees)[a] and Charge Distribution[b] for $Pt(PH_3)_2L$

L = O_2								L = C_2H_4							
		%[b]								%[b]							
Level	Energy	Pt	2 O	2 P	6 H	Major Pt basis fns[c]	Major O_2 basis fns[c]	Level	Energy	Pt	2 C	2 P	6 H_P	4 H_C	Major Pt basis fns[c]	Major C_2 basis fns[c]
$7b_2$	−0.0322	1	86	9	3		σ^*									
$6b_2$	−0.0788	41	33	22	4	d_{xy}	$\pi_\parallel^*$									
$3a_2$[d]	−0.2068	7	93	0	0		$\pi_\perp^*$	$5b_2$[d]	−0.1594	38	14	37	8	2	d_{xy}, p_y	$\pi_\parallel^*$
$5b_2$	−0.2394	10	58	27	6		$\pi_\parallel^*$	$8a_1$	−0.1604	37	40	16	6	0	$d_{x^2-y^2}$, p_x	$\pi_\parallel$
$8a_1$	−0.2417	55	15	21	9	$d_{x^2-y^2}$, p_x	$\pi_\parallel$	$7a_1$	−0.2108	80	4	13	4	0	d_{z^2}, s	
$7a_1$	−0.2466	81	7	10	3	d_{z^2}, s		$3b_1$	−0.2417	92	1	2	3	2	d_{xz}	
$3b_1$	−0.2617	68	27	2	3	d_{xz}	$\pi_\perp$	$3a_2$	−0.2503	88	2	3	4	3	d_{yz}	
$2a_2$	−0.3047	85	5	4	6	d_{yz}		$6a_1$	−0.2539	56	37	3	2	2	$d_{x^2-y^2}$, d_{z^2}	σ, $\pi_\parallel$
$6a_1$	−0.3376	41	25	25	9			$5a_1$	−0.3282	45	3	38	13	0		
$2b_1$	−0.3617	20	54	11	15	d_{xz}	$\pi_\perp$	$2a_2$	−0.3328	2	40	2	3	52		
$4b_2$	−0.3680	0	0	47	53			$4b_2$	−0.3376	42	2	36	20	1		
$1a_2$	−0.3733	5	0	46	50			$3b_2$	−0.3488	15	1	42	42	1		
$5a_1$	−0.3754	2	10	42	46			$1a_2$	−0.3500	4	2	44	49	2		
$1b_1$	−0.3800	12	9	38	41			$2b_1$	−0.3510	2	0	46	52	0		
$4a_1$	−0.3982	27	55	13	5	d_{z^2}, s	$\pi_\parallel$, σ	$4a_1$	−0.3516	5	2	44	47	1		
$3b_2$	−0.4008	56	12	25	7			$3a_1$	−0.3996	14	61	1	1	23	$d_{x^2-y^2}$, d_{z^2}	σ, $\pi_\parallel$
$3a_1$	−0.4255	23	73	2	1	$d_{x^2-y^2}$, d_{z^2}	σ, $\pi_\parallel$	$1b_1$	−0.4361	3	52	0	0	45		
$2b_2$	−0.6122	2	0	66	31			$2b_2$	−0.5468	2	57	0	0	41		
$2a_1$	−0.6152	2	0	66	31			$1b_2$	−0.5843	2	0	66	32	0		
$1b_2$	−0.7435	3	97	0	0			$2a_1$	−0.5863	2	0	66	32	0		
$1a_1$	−0.9588	5	95	0	0			$1a_1$	−0.6986	4	77	0	0	18		

[a] All levels up to −0.005 hartree except for diffuse Rydberg-state orbitals. These occur for $Pt(PH_3)_2(O_2)$ at −0.0593 ($4b_1$), −0.0502 ($9a_1$), and −0.0096 hartree ($10a_1$) and for $Pt(PH_3)_2(C_2H_4)$ at −0.0595 ($4b_1$), −0.0469 ($9a_1$), −0.0172 ($6b_2$), and −0.0136 hartree ($10a_1$). Only 5–14% of their charge is located within the atomic spheres. [b] Relative amounts of charge within the platinum, two oxygen, etc. spheres. They are the closest analogue of "atomic populations" from an LCAO calculation; there is no analogue of LCAO "overlap populations". More than 71% of the charge is within the atomic spheres for all levels tabulated except $7b_2$ (24%). [c] Spherical-harmonic basis functions contributing more than 10% of the Pt, O_2, or C_2 charge for the important Pt–O_2 and Pt–C_2H_4 levels are listed in order of decreasing importance. See Table II for explanation of symbols. [d] The highest occupied levels.

Table IV. Total Energies and Charge Distribution for $Pt(PH_3)_2L$[a]

	L = O_2	L = C_2H_4
Total energy	−181 66.5345	−180 95.2677
Virial ratio $-2T/V$[b]	1.000 06	1.000 05
Intersphere potential energy	−0.1786	−0.1777
Total charge in various regions		
Pt	77.05	77.30
O or C	7.76	5.69
P	14.31	14.31
H_P	1.01	1.01
H_C		0.93
Intersphere	2.21	2.22
Extramolecular	0.53	0.68
Estimated atomic charges[c]		
Pt	0.25+	0.07−
O or C	0.21−	0.00
P	0.36+	0.33+
H_P	0.09−	0.09−
H_C		0.01−

[a] Energies in hartrees; charges in electrons. [b] T = kinetic energy; V = potential energy. [c] See text for method of estimation.

Table V. Ionization Energies (eV)

Molecule	Level	Calcd IE[a]	Cor IE[b]	Exptl IE[c]
$Pt(PH_3)_2(O_2)$	$3a_2$	8.74		
	$5b_2$	9.14		
	$8a_1$	9.22		
	$7a_1$	9.60		
	$3b_1$	10.10		
	$2a_2$	11.47		
	Pt 4f	92.5	77.5	73.2 ± 0.1
	P 2p	132.3	132.8	132.0 ± 0.1
	O 1s	529.0	529.6	531.2 ± 0.1
$Pt(PH_3)_2(C_2H_4)$	Pt 4f	90.5	75.5	72.7 ± 0.3
	P 2p	131.2	131.7	131.5 ± 0.2
	C 1s	283.0	283.2	283.3 ± 0.2

[a] Calculated using the transition-state procedure[9b] and the relation 1 hartree = 27.2116 eV. [b] Corrected for relativistic effects (see text). Both the corrected and experimental Pt 4f values are for the $4f_{7/2}$ component. Both P 2p values are weighted averages of the $2p_{1/2}$ and $2p_{3/2}$ components. [c] Average of two and three independent determinations for the O_2 and C_2H_4 complexes, respectively, by ESCA.[24-27] Estimated errors are the largest deviation of the measured values from the average.

of valence electrons within each atomic sphere. This is clearly a very approximate technique; I consider only the relative values for the two molecules, not the absolute numbers, likely to be consistently reliable. However, for iron–sulfur complexes, comparison of numbers obtained by this scheme and a more accurate partitioning method under development (based on atomic-sphere-surface charges[21]) show agreement within 0.01–0.31 electron for all atoms.[22] Also, the sum total of experimental data indicates a charge of about 0.3+ for phosphorus in most phosphine complexes, usually greater than that of the metal,[23] consistent with the values in Table IV.

Ionization energies for both molecules appear in Table V. Calculated values (which include the effects of orbital relaxation[9b]) are given for the lowest six valence levels of $Pt(PH_3)_2(O_2)$ and for core levels accessible by ESCA for both molecules. There have been several independent experimental determinations for the core levels[24-27] but none for the valence levels. Calculated core energies corrected for relativistic effects are also given. For the Pt $4f_{7/2}$ level, the corrections are the explicit difference between nonrelativistic[28] and relativistic[29] Pt atom SCF–Xα values (both for α = 1); for the other levels, the perturbation theory corrections of Herman and Skillman for the free-atom levels[28] (again for α = 1) were used. Clearly, both types of correction can only be approximately right for the molecular levels.

Discussion

Pt–O_2 and Pt–C_2H_4 Bonding. Because $Pt(PPh_3)_2(O_2)$ is normally[12] prepared from the d^{10} complex $Pt(PPh_3)_3$ and neutral O_2 and is being compared with $Pt(PPh_3)_2(C_2H_4)$, it

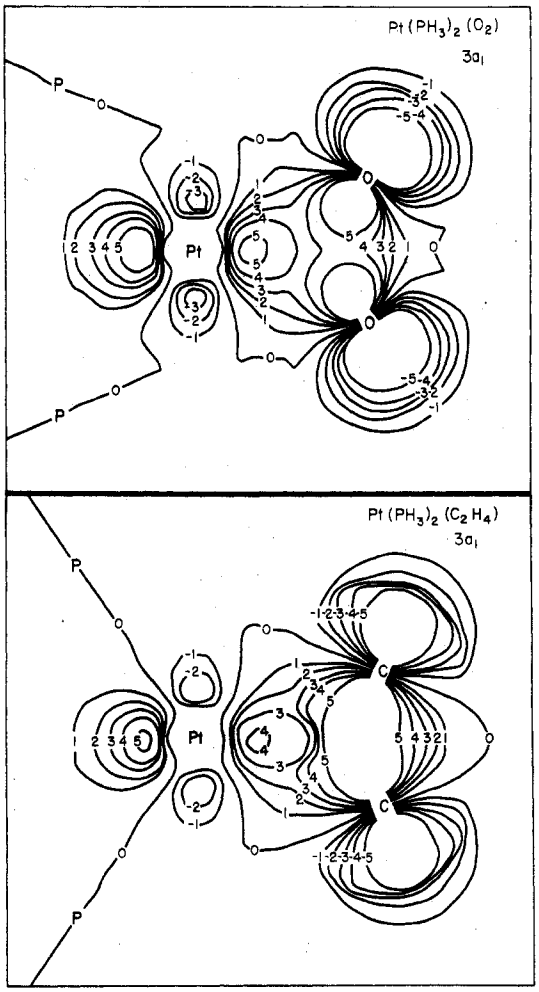

Figure 2. Contour maps of the wave functions for the most important Pt–O_2 and Pt–C_2H_4 bonding orbitals. These and all subsequent maps are in the *xy* (molecular) plane; interior contours close to the atomic centers are always omitted for clarity. The contour values are 0, ±1, ±2, ±3, ±4, ±5 for 0, ±0.05, ±0.075, ±0.10, ±0.125, ±0.160, respectively.

is useful to discuss the results in the language of the Dewar–Chatt model, which views the bonding as a combination of "forward-donation" from O–O or C–C bonding orbitals to the metal and "back-donation" from the metal into π^*-antibonding orbitals of the neutral ligand.

The basic features of the bonding are clear from Figure 1. In the O_2 complex, the lower three orbitals are mainly ligand σ and π, with, however, 20–30% metal character. Next come four largely Pt 5d orbitals. The two highest occupied levels, mainly O_2 π^*, have very little Pt character. There are two rather high-energy unoccupied orbitals, the first mainly Pt $5d_{xy}$ and the second O_2 σ^*.

The same general picture holds for the C_2H_4 complex—except that there are no out-of-plane π and π^* orbitals—until one reaches the uppermost levels. Instead of a filled, essentially $\pi_{\|}^*$ b_2 orbital at lower energy and an empty, mainly d_{xy} b_2 orbital at higher energy, there is a single filled level, mainly d_{xy}, but with significant π^* character. To understand how this comes about, consider the two molecules as being formed from a $Pt(PH_3)_2$ fragment and either O_2 or C_2H_4. Since d_{xy} is the metal orbital which points most directly at the PH_3 ligands, the fragment will have a single high-lying filled orbital, mainly d_{xy}. The important point is that the O_2 π^* orbital is much lower in energy than this fragment donor orbital, while the C_2H_4 π^* orbital is higher in energy. The necessary qualitative

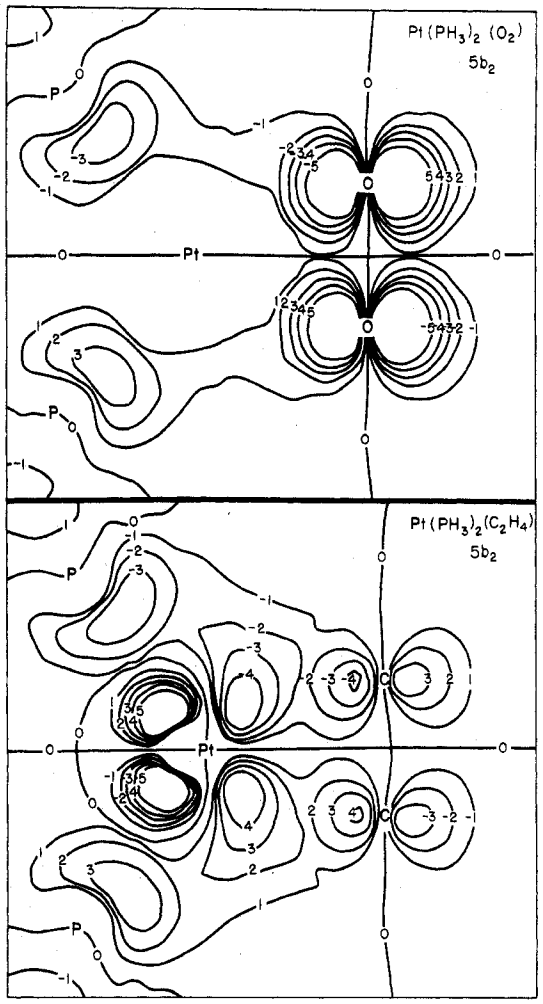

Figure 5. Contour maps of the wave functions for the main Pt–O_2 and Pt–C_2H_4 back-bonding orbitals, with the same contour values as Figure 2.

result is that the lower energy, filled orbital of the interaction will be mainly π^* in the O_2 case and mainly d_{xy} in the C_2H_4 case. The mostly π^* orbital in the C_2H_4 case, destabilized by the interaction, is not even found as a localized orbital at negative energy. Thus for O_2 we have an approximately d^8 peroxide complex—four of the five mainly d orbitals filled and both mainly π^* orbitals filled—while for C_2H_4 we have an approximately d^{10} complex—all five mainly d orbitals filled.

Inspection of wave function contour maps reveals more details. Pt–O_2 and Pt–C_2H_4 covalent interaction is mainly "forward-donation", involving mixing of $d_{x^2-y^2}$ and d_{z^2} with *both* σ- and π-bonding orbitals. As found for Zeise's anion, $[PtCl_3(C_2H_4)]^-$, by the SCF-Xα-SW method,[30] there are three main metal–ligand covalent bonding orbitals for both $Pt(PH_3)_2(O_2)$ and $Pt(PH_3)_2(C_2H_4)$, all of a_1 symmetry. The striking feature of the most important of these, $3a_1$ (see Figure 2), is that the ligand contribution is much more from the σ than the π orbital. The importance of σ-orbital participation has been overlooked in past qualitative treatments of the bonding in O_2 and C_2H_4 complexes.[31] The σ and π functions contribute about equally to the second important bonding orbital depicted in Figure 3, but in the third (Figure 4) the π function is dominant.

Figure 5 shows the highest filled in-plane levels, the main "back-bonding" orbitals. For the O_2 complex there is almost no metal contribution; the orbital is mainly localized on O_2. For the C_2H_4 complex the orbital is mainly Pt $5d_{xy}$, but there is appreciable overlap with the ligand π^* function. Thus we

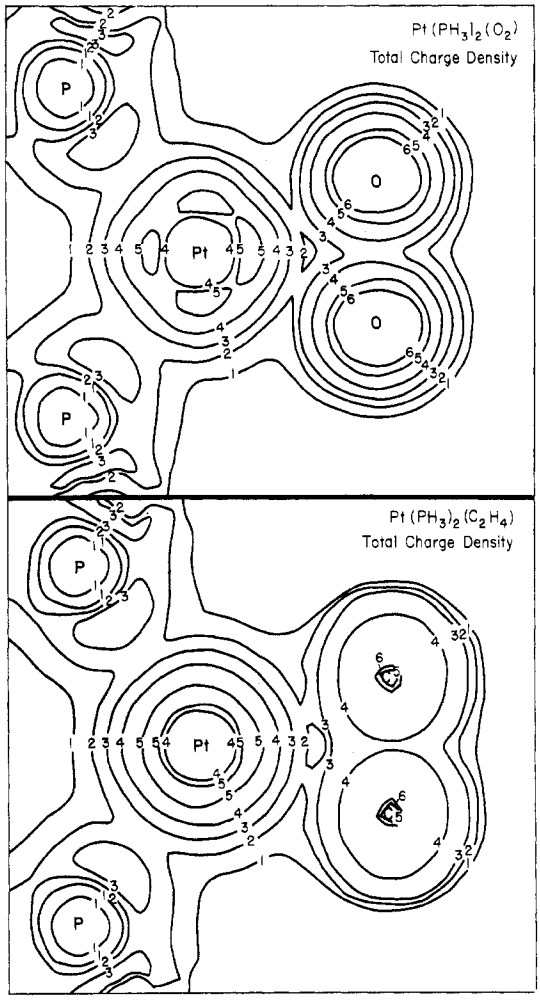

Figure 6. Contour maps of the total valence charge densities of the two complexes. The contour values are 1, 2, 3, 4, 5, 6 for 0.014, 0.028, 0.042, 0.070, 0.140, 0.210, respectively.

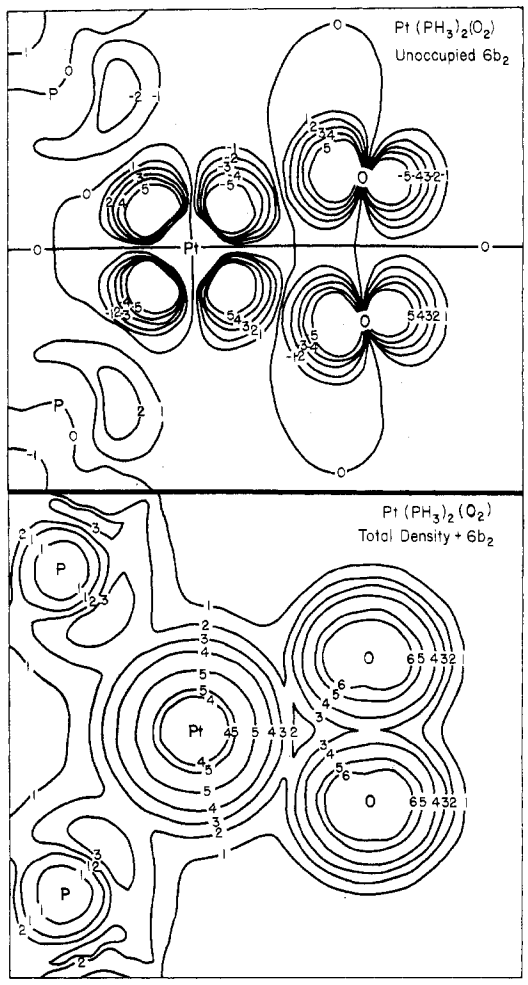

Figure 7. Contour maps of the first unoccupied orbital of $Pt(PH_3)_2(O_2)$ and the total charge density including this orbital. The contour values are the same as Figures 2 and 6, respectively.

have the interesting result that, in bonding to Pt, O_2 acquires much more π^*-orbital density than does C_2H_4—but the back-bonding is more *covalent* for C_2H_4. The simplest way to describe the formation of the Pt–O_2 bond is as an initial two-electron charge transfer from Pt to O_2, followed by strong covalent mixing of peroxide σ- and π-*bonding* orbitals with mainly 5d orbitals of $Pt(PH_3)_2^{2+}$. The two filled O_2^{2-} π^* orbitals remain essentially localized on the ligand.

This result for Pt–O_2 interaction should be viewed in a wider context. General discussions of metal-to-ligand back-bonding have not sufficiently emphasized the fact that there can be a buildup of electrons in ligand π^* orbitals purely by inductive charge transfer from metal to ligand, without covalent overlap with metal dπ orbitals. Common experimental criteria for back-bonding, such as lowered CO stretching frequencies for carbonyls and increased C–C distances for ethylene complexes, merely reflect increased population of ligand π^* orbitals, which will result from either ionic or covalent back-bonding. In fact, as Chatt and co-workers showed in an interesting recent paper,[23] the sum total of available data on π-acid complexes clearly indicates that bonds to CO, NO, N_2, etc. are usually quite polar in the direction $M^{\delta+}$–$L^{\delta-}$ (although covalent dπ–π^* interaction is also usually present). There are probably other ligands besides O_2—e.g., $C_2(CN)_4$—for which, at least in some situations, the ionic component of the back-bond is overwhelmingly dominant.

Figure 6 shows the total valence charge density for the two molecules in the molecular plane. There is probably no simpler illustration that the O_2 complex is essentially d^8 whereas the C_2H_4 complex is essentially d^{10}. In the O_2 case the Pt atom would be essentially spherical—i.e., closed shell—except for missing density in the d_{xy}-orbital region; in the C_2H_4 case it is nearly spherical. Moreover, in Figure 7 we see the mainly d_{xy} LUMO of the O_2 complex and what the charge density would be if it were occupied. The Pt region looks remarkably like that in the ethylene complex.

Another interesting feature of the charge density maps is that the maximum density in the metal–ligand bonds lies nearly along the lines of centers between the Pt and the individual O or C atoms rather than between Pt and the O–O or C–C midpoint. This supports the view that O_2 and C_2H_4 occupy two coordination positions rather than one.

It is clear from Figure 6 that overall in-plane covalent bonding of the two ligands to Pt is comparable in strength, consistent with the fact that the Pt–O and Pt–C distances differ by exactly the difference between the covalent radii of oxygen and carbon. The total Pt–O_2 bond, however, appears stronger than the Pt–C_2H_4 bond, since it includes in addition the ionic $Pt^{\delta+}$–$O_2^{\delta-}$ attraction. Consistently, $Pt(PPh_3)_2(C_2H_4)$ dissociates appreciably in benzene, while $Pt(PPh_3)_2(O_2)$ remains intact.[13]

Finally, interaction of the out-of-plane O_2 π and π^* orbitals with the metal is not very important. The mainly $\pi_\perp$ orbital, $2b_1$, has 20% Pt character (Table III), but inspection of contour maps shows that Pt $5d_{xz}$–O_2 $\pi_\perp$ overlap in the orbital is small, and in any case its effect is largely canceled by corresponding antibonding d_{xz}–$\pi_\perp$ interaction in the higher energy $3b_1$ level.

As for the $\pi_\perp$* orbital, it remains strongly localized on O_2 as the HOMO, $3a_2$.

Comparison with Experiment. The spectral band responsible for the orange color of $Pt(PPh_3)_2(O_2)$, the only one clearly observed before phenyl group absorption[32] obscures the spectrum, maximizes at 29.8×10^3 cm^{-1} (ϵ 1100). The calculations predict the lowest electronic transition of $Pt(PH_3)_2(O_2)$ to be the allowed $3a_2 \rightarrow 6b_2$ excitation, corresponding to O_2 $\pi^* \rightarrow$ Pt $5d_{xy}$ charge transfer, with an energy of 31.8×10^3 cm^{-1}. No other transitions are predicted below 39×10^3 cm^{-1}. Moreover, our failure to find localized excited levels of $Pt(PH_3)_2(C_2H_4)$ below −0.005 hartree indicates that this molecule should have no strong transitions below about 34×10^3 cm^{-1}. The spectrum of $Pt(PPh_3)_2(C_2H_4)$ in C_2H_4-saturated benzene,[33] believed to be due to the undissociated complex, shows its first maximum at 34.7×10^3 cm^{-1}.

The x-ray photoelectron spectra of $Pt(PPh_3)_2L$, L = PPh_3, C_2H_2, C_2H_4, O_2, Cl_2, have been interpreted to indicate a significant positive charge on Pt in the O_2 complex, greater than in the C_2H_4 complex.[24] This agrees with our formulation of the bonding and with the roughly estimated atomic charges in Table IV. Moreover, as shown in Table V, both the calculated Pt 4f and P 2p ionization energies for the O_2 complex are greater than for the C_2H_4 complex, in agreement with experiment. The calculated P 2p, O 1s, and C 1s energies are all within 0.4% of experiment, even without correction for relativistic effects. For the Pt 4f levels, however, such effects are clearly very important. This raises the question of how much the calculated mainly Pt valence levels might be in error due to this factor. Explicit comparison of the Pt atom 5d orbital energy from relativistic and nonrelativistic SCF–Xα calculations[34] shows that the correction for even a purely 5d molecular level would be a downshift of only about 0.02 hartree. This would affect neither the ordering of the levels nor any of the conclusions about bonding.

Many of the features of electronic structure calculated here for $Pt(PH_3)_2(O_2)$ are probably applicable to most other chelated-O_2 complexes, especially the six-coordinate complexes of Co, Rh, and Ir. In a recent review,[3] Vaska drew on all available data to argue convincingly for the generality of the peroxo formulation. Bosnich et al. have shown[4] that the same complexes originally made from Co^I and O_2 are easily prepared from Co^{III} and O_2^{2-}. Gray et al. pointed out[5] that the electronic spectra of "Co^I–O_2" and Co^{III}–CO_3^{2-} complexes are virtually identical.

The six-coordinate complexes differ from $Pt(PH_3)_2(O_2)$ principally in having two less mainly metal electrons and two additional z-axis ligands. Their energy-level diagrams should therefore differ from the Pt case in having the mainly d_{z^2} orbital ($7a_1$) elevated in energy to become the lowest or second lowest unoccupied orbital. One-electron electrolytic reduction of $Ir(Ph_2PCH_2CH_2PPh_2)(O_2)^+$ leads to dissociation of O_2, suggesting that the LUMO is strongly Pt–O_2 antibonding—i.e., as we find for $Pt(PH_3)_2(O_2)$, mainly d_{xy} rather than d_{z^2}.[35]

In moving from the third-row metals Pt and Ir to the first-row metal Co, one might expect a decrease in ligand field splitting and covalency, possibly making the mainly d rather than mainly π^* orbitals the highest occupied ones and leading to lower energy electronic transitions than in $Pt(PH_3)_2(O_2)$. Indeed, the first two bands for $Co(2{=}phos)_2(O_2)^+$ lie at 21×10^3 and 26×10^3 cm^{-1} and were assigned by Gray et al. to d–d transitions.[5]

In-Plane vs. Perpendicular Coordination for C_2H_4 and O_2. The most striking difference in structure between the d^8 complex $[PtCl_3(C_2H_4)]^-$ and the d^{10} complex $Pt(PPh_3)_2(C_2H_4)$ is that the C–C bond lies perpendicular to the plane in the former and lies in the plane in the latter, as shown by

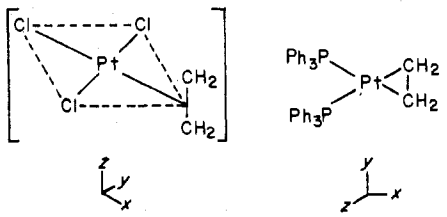

The calculations explain the in-plane coordination simply in terms of the relative availability of the in-plane (d_{xy}) and out-of-plane (d_{xz}) back-bonding orbitals of the fragment $Pt(PPh_3)_2$. As pointed out above, the d_{xy} orbital will be high in energy and "pushed" toward the C_2H_4, due to its strong Pt–P antibonding character. Both factors favor its interaction with the very high-energy π^* orbital. There is no comparable destabilizing or directionalizing effect on the d_{xz} orbital. The in-plane ethylene conformation is thus largely due to the very different trans influence of the PPh_3 ligand on the d_{xy} and d_{xz} orbitals.

In $[PtCl_3(C_2H_4)]^-$, however, the potential in-plane back-bonding orbital lies *between* the Cl ligands and thus is unlikely to be very differently perturbed by them than the out-of-plane orbital. The ethylene, with little basis on which to choose, adopts the sterically more favorable perpendicular position. Back-bonding is much weaker in the absence of the ligand trans influence. These conclusions are confirmed by the C–C distance of 1.375 (4) Å[36] [only 0.038 Å longer than in free ethylene; cf. 1.43 Å in $Pt(PPh_3)_2(C_2H_4)$], the easy rotation of C_2H_4 around L_3Pt^{II}–C_2H_4 bonds,[37] ^{13}C NMR experiments which indicate the Pt^{II}–C_2H_4 bond to involve largely forward-donation,[38] and SCF–Xα–SW calculations on $[PtCl_3(C_2H_4)]^-$.[30]

For the O_2 complex, significant covalent back-bonding appears absent, but the usual ligand field stabilization energy arguments favoring planar over pseudotetrahedral coordination for four-coordinate d^8 complexes apply. The planar structure is also favored by the character of the "forward-donation" orbitals of a_1 symmetry. Although interaction with the Pt $5d_{x^2-y^2}$ orbital should not greatly differ for in-plane and perpendicular ligand orientations, overlap with the $5d_{x^2}$ "donut" is clearly more effective in the plane. Figure 3 shows that such overlap is indeed a significant component of the bonding in $Pt(PH_3)_2(O_2)$ (but, interestingly, not in $Pt(PH_3)_2(C_2H_4)$).

Monodentate vs. Chelating O_2. Similar considerations apply to the problem of why, independently of whether one considers bound O_2 to be neutral, superoxo, or peroxo, monodentate coordination is found in some situations and chelating in others. There have been several discussions of this point based essentially on Walsh diagrams generated at varying levels of sophistication.[39-42] I have one simple, limited observation to add: in the known structures of coordination number 6 or less, the presence of monodentate or chelating O_2 is consistent with the expected influence of ligands trans to the O_2. One ligand is found directly trans to monodentate O_2 and two ligands are found roughly trans to the two oxygen atoms of chelated O_2. The Co^{III} complexes depicted in **4** and **5** provide an example.[43,44] The main Co–O_2 bonding interaction in **4** is Co $3d_{z^2}$–O_2 π^*, while in **5** Co $3d_{z^2}$–O_2 $\sigma\pi$ and Co $3d_{xz}$–O_2 π^* should be considered.[39,41] The point is that in both **4** and **5**

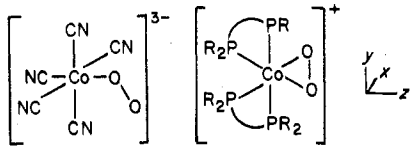

4 **5**

the trans donor ligands point at, and thus elevate the energy of, just those metal orbitals which interact with the relatively high-energy O_2 π^* orbital, thereby improving that interaction. In **5** they fail to elevate the $3d_{z^2}$ orbital, thus favoring its interaction with the relatively low-energy O_2 $\sigma\pi$ set. A striking illustration of this trans influence is provided by the recently reported complexes Cr(TPP)(py)(O_2)[45] and Mn(TPP)(O_2)[46] (TPP = tetraphenylporphyrin), which appear to have the basic structures shown below—i.e., similar to **4** and **5** above, respectively.

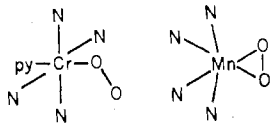

Both appear to be d^3 systems (Cr^{III}–O_2^- and Mn^{IV}–O_2^{2-}, respectively), and both are prepared starting from M(TPP)(py)—but the Mn compound loses the pyridine ligand in the process of attaining the chelated-O_2 structure. The x-ray structure of another porphyrin complex having completely analogous geometry to that proposed for the Mn system, Ti(OEP)(O_2), has recently appeared.[47]

Reactivity of Chelated-O_2 Complexes. Most discussions of reactivity in terms of calculations focus on the HOMO and LUMO of the molecule in question. For the O_2 complex, the HOMO is well separated in energy from lower levels and strongly localized on the O_2 unit as the perpendicular π^* orbital. There is a large energy gap between it and the mainly Pt $5d_{xy}$ LUMO. Such a diagram is characteristic of a nucleophile; the molecule should act as a donor through the O_2 unit. This is just what is observed: a survey of known reactions of $Pt(PPh_3)_2(O_2)$ leads to the conclusion that the reactivity is greatest in cases where the O_2 moiety acts formally as a nucleophile.[7] Of course, the mechanisms of these reactions are generally unknown, so "formally" may be an important word here. There is at least one known structure, however, where the perpendicular π^* orbital is "caught in the act" of serving as a donor (**6**). As suggested in the structural paper,[48]

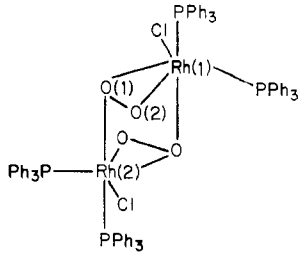

6

such donation is the only reasonable explanation for the molecular geometry. The angle $O_2O_1Rh_2$ = 102.5 (3)° is indeed perfectly consistent with the expected electron distribution in the π^* orbital, slightly swept back from the O–O region.

The only reaction which seems universal for all group 8 chelated-O_2 complexes, and also the one for which there is the clearest indication of mechanism, is addition of SO_2 to give coordinated sulfate, exemplified below for $Pt(PPh_3)_2(O_2)$.

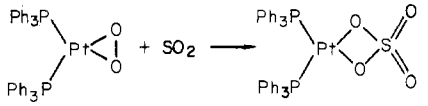

From ^{18}O-labeling studies of the $Ir(PPh_3)_2(CO)(Cl)(O_2)$–SO_2 system, SO_2 insertion into one M–O bond has been proposed as a likely first step for this reaction[49]

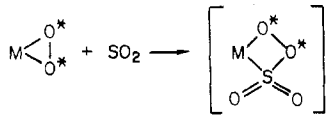

The energy-level diagram for $Pt(PH_3)_2(O_2)$ suggests how this might occur in a concerted fashion

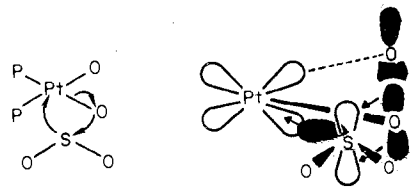

electron shift interacting orbitals (black = filled, white = empty)

The LUMO of SO_2, a p-type, mainly sulfur orbital perpendicular to the plane, is perfectly set up to accept electrons from the π^* HOMO of the complex. At the same time, the in-plane, mainly sulfur HOMO of SO_2 can donate to the mainly Pt $5d_{xy}$ LUMO of the complex. This LUMO is, in fact, strongly antibonding with respect to the Pt–O_2 bond (see Figure 7), so that population of it should help rupture this bond.

$Pt(PPh_3)_3$ is a homogeneous catalyst for oxidation of Ph_3P to Ph_3PO, and $Pt(PPh_3)_2(O_2)$ has been established as the important catalytic intermediate.[13] The mechanism supported by kinetic studies for the critical step in this process is shown below (PPh_3 represented by P for clarity).

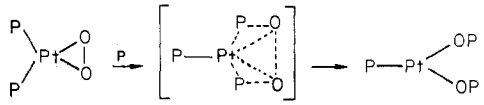

This step formally represents a transfer of four electrons into the PtO_2 system; i.e., it converts Pt^{II} to Pt^0 and severs the remaining O–O bond in O_2^{2-}. Our calculated energy-level diagram does indeed predict the likelihood of such processes, for there are exactly two well-defined unoccupied orbitals of $Pt(PH_3)_2(O_2)$ at negative energies, one mainly Pt $5d_{xy}/O_2$ $\pi_{\|}^*$ and the other essentially O_2 σ^*. The combination of these two orbitals, both belonging to the b_2 representation, favors just the sort of symmetrical attraction of two PPh_3 ligands proposed in the preceding bracketed transition state.

Pt→P Back-Bonding. There are no orbitals in either complex to which the phosphorus contribution is mainly from 3d functions. However, as shown in Table VI, there is a significant change in hybridization of the phosphorus bonding functions upon complexation to Pt, amounting to replacement of s by d character. This effect is greatest in the high-lying $8a_1$ orbital, where the d component reaches 20–30% of the total phosphorus contribution. The $8a_1$ orbital contains much more Pt than P character; to the extent that the P character is 3d, it thus represents Pt(5d)→P(3d) back-bonding.

There has been much discussion of whether the shortening of M–P bonds from the sum of covalent radii invariably observed in phosphine complexes is due to π back-bonding or merely reflects increased P 3s character in the M–P σ bond.[50-52] The present results suggest the unified view that the bond shortening and related phenomena reflect some, but not always the same, sort of change in phosphorus hybridization upon complexation to metals. For PH_3 bonding to Pt, this change appears to be essentially replacement of s by d character, with the bonding functions remaining mainly 3p. This does not mean that the same type or magnitude of change will occur for PR_3 ligands where R is more electronegative, or more complex, than H. In particular, a rapid increase in 3s character of the complexed-PR_3 donor orbital as R is made more electronegative has been demonstrated experimentally.[52] We plan additional calculations on PR_3 complexes with varying

Table VI. Spherical-Harmonic Character of Phosphorus-Sphere Contribution to PH_3 Lone-Pair Orbital and Complex Pt-P Bonding Orbitals

Molecule	Orbital	Phosphorus-sphere character[a] % s	% p	% d
PH_3	$2a_1$	21	79	0
$Pt(PH_3)_2(O_2)$	$3b_2$	3	89	8
	$6a_1$	8	85	7
	$8a_1$	13	64	23
	Av	8	79	13
$Pt(PH_3)_2(C_2H_4)$	$4b_2$	5	85	10
	$5a_1$	6	89	5
	$8a_1$	18	53	29
	Av	10	76	15

[a] For PH_3, the $2a_1$ orbital as a whole is 81% phosphorus and 19% hydrogen. See Table III for the extent of phosphorus contribution to the orbitals listed above for the complexes.

R to help resolve these questions.

Acknowledgment. I thank the National Science Foundation for support of this research.

Registry No. $Pt(PH_3)_2(O_2)$, 53195-21-4; $Pt(PH_3)_2(C_2H_4)$, 31941-73-8; PH_3, 7803-51-2.

Supplementary Material Available: Figures 3 and 4 showing contour maps of the wave functions for the second and third important $Pt-O_2$ and $Pt-C_2H_4$ bonding orbitals (2 pages). Ordering information is given on any current masthead page.

References and Notes

(1) (a) J. P. Collman, J. I. Brauman, and K. S. Suslick, *J. Am. Chem. Soc.*, **97**, 7185 (1975); (b) J. P. Collman, R. R. Gagne, C. A. Reed, T. R. Halbert, G. Lang, and W. T. Robinson, *ibid.*, **97**, 1427 (1975).
(2) J. H. Dawson, R. H. Holm, J. R. Trudell, G. Barth, R. E. Linder, E. Bunnenberg, C. Djerassi, and S. C. Tang, *J. Am. Chem. Soc.*, **98**, 3707 (1976), and references therein.
(3) L. Vaska, *Acc. Chem. Res.*, **9**, 175 (1976). For other reviews of dioxygen complexes see (a) J. S. Valentine, *Chem. Rev.*, **73**, 235 (1973); (b) V. J. Choy and C. J. O'Connor, *Coord. Chem. Rev.*, **9**, 145 (1972).
(4) (a) B. Bosnich, W. G. Jackson, S. T. D. Lo, and J. W. McLaren, *Inorg. Chem.*, **13**, 2605 (1974); (b) B. Bosnich, H. Boucher, and C. Marshall, *ibid.*, **15**, 634 (1976).
(5) V. M. Miskowski, J. L. Robbins, G. S. Hammond, and H. B. Gray, *J. Am. Chem. Soc.*, **98**, 2477 (1976).
(6) (a) M. Laing, M. J. Nolte, and E. Singleton, *J. Chem. Soc., Chem. Commun.*, 660 (1975); (b) M. J. Nolte, E. Singleton, and M. Laing, *J. Am. Chem. Soc.*, **97**, 6396 (1975).
(7) S. L. Regen and G. M. Whitesides, *J. Organomet. Chem.*, **59**, 293 (1973).
(8) K. Fukui and S. Inagaki, *J. Am. Chem. Soc.*, **97**, 4445 (1975).
(9) (a) K. H. Johnson, *Annu. Rev. Phys. Chem.*, **26**, 39 (1975); (b) J. C. Slater, "Quantum Theory of Molecules and Solids", Vol. 4, McGraw-Hill, New York, N.Y., 1974.
(10) C. J. Nyman, C. E. Wymore, and G. Wilkinson, *J. Chem. Soc. A*, 561 (1968).
(11) P. T. Cheng, C. D. Cook, S. C. Nyburg, and K. Y. Wan, *Can. J. Chem.*, **49**, 3772 (1971).
(12) P. J. Hayward, D. M. Blake, G. Wilkinson, and C. J. Nyman, *J. Am. Chem. Soc.*, **92**, 5873 (1970).
(13) (a) J. P. Birk, J. Halpern, and A. L. Pickard, *J. Am. Chem. Soc.*, **90**, 4491 (1968); (b) J. Halpern and A. L. Pickard, *Inorg. Chem.*, **9**, 2798 (1970).
(14) P. T. Cheng and S. C. Nyburg, *Can. J. Chem.*, **50**, 912 (1972).
(15) J. G. Norman, Jr., *J. Am. Chem. Soc.*, **96**, 3327 (1974).
(16) (a) K. Kuchitzer, *J. Mol. Spectros.*, **7**, 399 (1961); (b) M. H. Sivertz and R. E. Weston, Jr., *J. Chem. Phys.*, **21**, 898 (1953).
(17) L. E. Sutton, Ed., *Chem. Soc., Spec. Publ.*, **18**, S19s (1965).
(18) K. Schwarz, *Phys. Rev. B*, **5**, 2466 (1972); *Theor. Chim. Acta*, **34**, 225 (1974).
(19) J. C. Slater, *Int. J. Quantum Chem.*, **7S**, 533 (1973).
(20) (a) J. G. Norman, Jr., *J. Chem. Phys.*, **61**, 4630 (1974); (b) J. G. Norman, Jr., *Mol. Phys.*, **31**, 1191 (1976).
(21) D. A. Case and M. Karplus, *Chem. Phys. Lett.*, **39**, 33 (1976).
(22) D. A. Case, personal communication.
(23) J. Chatt, C. E. Elson, N. E. Hooper, and G. J. Leigh, *J. Chem. Soc., Dalton Trans.*, 2392 (1975).
(24) C. D. Cook, K. Y. Wan, U. Gelius, K. Hamrin, G. Johannson, E. Olsson, H. Siegbahn, C. Nordling, and K. Siegbahn, *J. Am. Chem. Soc.*, **93**, 1904 (1971).
(25) D. T. Clark, D. B. Adams, and D. Briggs, *Chem. Commun.*, 602 (1971).
(26) W. M. Riggs, *Anal. Chem.*, **44**, 830 (1972).
(27) R. Mason, D. M. P. Mingos, G. Rucci, and J. A. Connor, *J. Chem. Soc., Dalton Trans.*, 1729 (1972).
(28) F. Herman and S. Skillman, "Atomic Structure Calculations", Prentice-Hall, Englewood Cliffs, N.J., 1963.
(29) D. Liberman, J. T. Waber, and D. T. Cromer, *Phys. Rev.* [*Sect.*] *A*, **137**, 27 (1965).
(30) N. Rösch, R. P. Messmer, and K. H. Johnson, *J. Am. Chem. Soc.*, **96**, 3855 (1974).
(31) F. R. Hartley, *Angew. Chem., Int. Ed. Engl.*, **11**, 596 (1972).
(32) H. H. Jaffe and M. Orchin, "Theory and Applications of Ultraviolet Spectroscopy", Wiley, New York, N.Y., 1962, p 498.
(33) Y. Soma, *Bull. Chem. Soc. Jpn.*, **44**, 3233 (1971).
(34) J. T. Waber and F. W. Averill, *J. Chem. Phys.*, **60**, 4466 (1974).
(35) B. K. Teo, A. P. Ginsberg, and J. C. Calabrese, *J. Am. Chem. Soc.*, **98**, 3027 (1976).
(36) R. A. Love, T. F. Koetzle, G. J. B. Williams, L. C. Andrews, and R. Bau, *Inorg. Chem.*, **14**, 2653 (1975).
(37) C. E. Holloway, G. Hulley, B. F. G. Johnson, and J. Lewis, *J. Chem. Soc. A*, 53 (1969); 1653 (1970).
(38) D. G. Cooper and J. Powell, *Inorg. Chem.*, **15**, 1959 (1976).
(39) A. Dedieu, M. M. Rohmer, and A. Veillard, *J. Am. Chem. Soc.*, **98**, 5789 (1976).
(40) D. M. P. Mingos, *Nature* (*London*), *Phys. Sci.*, **230**, 153 (1971).
(41) B. K. Teo and W. K. Li, *Inorg. Chem.*, **15**, 2005 (1976).
(42) R. Hoffmann, M. M. L. Chen, and D. L. Thorn, *Inorg. Chem.*, **16**, 503 (1977).
(43) L. D. Brown and K. N. Raymond, *Inorg. Chem.*, **14**, 2595 (1975).
(44) N. W. Terry, E. L. Amma, and L. Vaska, *J. Am. Chem. Soc.*, **94**, 653 (1972).
(45) S. K. Cheung, C. J. Grimes, J. Wong, and C. A. Reed, *J. Am. Chem. Soc.*, **98**, 5028 (1976).
(46) B. M. Hoffman, C. J. Weschler, and F. Basolo, *J. Am. Chem. Soc.*, **98**, 5473 (1976).
(47) R. Guilard, M. Fontesse, P. Fournari, C. Lecomte, and J. Protas, *J. Chem. Soc., Chem. Commun.*, 161 (1976).
(48) M. J. Bennett and P. B. Donaldson, *J. Am. Chem. Soc.*, **93**, 3307 (1971).
(49) J. Valentine, D. Valentine, Jr., and J. P. Collman, *Inorg. Chem.*, **10**, 219 (1971).
(50) J. G. Verkade, *Coord. Chem. Rev.*, **9**, 1 (1972).
(51) H. J. Plastas, J. M. Stewart, and S. O. Grim, *Inorg. Chem.*, **12**, 265 (1973).
(52) B. B. Wayland and M. E. Abd-Elmageed, *J. Am. Chem. Soc.*, **96**, 4809 (1974).